# Syntheses and Structural Characterization of Dinuclear and Tetranuclear Iron(III) Complexes with Dinucleating Ligands and Their Reactions with Hydrogen Peroxide‡

**Lars Westerheide, Felizitas K. Müller, Roberto Than, and Bernt Krebs*,§**

Anorganisch-Chemisches Institut, Universität Münster, Wilhelm-Klemm-Strasse 8, 48149 Münster, Germany

**Jens Dietrich and Siegfried Schindler*,||**

Institut für Anorganische Chemie, Universität Erlangen-Nürnberg, Egerlandstrasse 1, 91058 Erlangen, Germany

*Received August 15, 2000*

The iron(III) complexes $[Fe_2(HPTB)(\mu\text{-}OH)(NO_3)_2](NO_3)_2\cdot CH_3OH\cdot 2H_2O$ (**1**), $[Fe_2(HPTB)(\mu\text{-}OCH_3)(NO_3)_2](NO_3)_2\cdot 4.5CH_3OH$ (**2**), $[Fe_2(HPTB)(\mu\text{-}OH)(OBz)_2](ClO_4)_2\cdot 4.5H_2O$ (**3**), $[Fe_2(N\text{-}EtOH\text{-}HPTB)(\mu\text{-}OH)(NO_3)_2](ClO_4)(NO_3)\cdot 3CH_3OH\cdot 1.5H_2O$ (**4**), $[Fe_2(5,6\text{-}Me_2\text{-}HPTB)(\mu\text{-}OH)(NO_3)_2](ClO_4)(NO_3)\cdot 3.5CH_3OH\cdot C_2H_5OC_2H_5\cdot 0.5H_2O$ (**5**), and $[Fe_4(HPTB)_2(\mu\text{-}F)_2(OH)_4](ClO_4)_4\cdot CH_3CN\cdot C_2H_5OC_2H_5\cdot H_2O$ (**6**) were synthesized (HPTB = *N*,*N*,*N*′,*N*′-tetrakis(2-benzimidazolylmethyl)-2-hydroxo-1,3-diaminopropane, N-EtOH-HPTB = *N*,*N*,*N*′,*N*′-tetrakis-(*N*″-(2-hydroxoethyl)-2-benzimidazolylmethyl)-2-hydroxo-1,3-diaminopropane, 5,6-$Me_2$-HPTB = *N*,*N*,*N*′,*N*′-tetrakis(5,6-dimethyl-2-benzimidazolylmethyl)-2-hydroxo-1,3-diaminopropane). The molecular structures of **2**−**6** were established by single-crystal X-ray crystallography. Iron(II) complexes with ligands similar to the dinucleating ligands described herein have been used previously as model compounds for the dioxygen uptake at the active sites of non-heme iron enzymes. The same metastable ($\mu$-peroxo)diiron(III) adducts were observed during these studies. They can be prepared by adding hydrogen peroxide to the iron(III) compounds **1**−**6**. Using stopped-flow techniques these reactions were kinetically investigated in different solvents and a mechanism was postulated.

## Introduction

Metalloproteins such as methane monooxygenase (MMO), ribonucleotide reductase (RR), hemerythrin (Hr), and purple acid phosphatases (PAPs), the X-ray structures of which are all available, belong to the class of non-heme diiron enzymes.[1−10] They are capable of binding and activating dioxygen.[11−13] Their active sites contain either a mixed-valent Fe(II)Fe(III) core (mammalian PAPs) or an Fe(II)Fe(II) center (MMO, RR, Hr) which is directly involved in the reaction with dioxygen. Diiron(III) peroxo species are considered to play an important role in the catalytic cycles of these enzymes, but intricate mechanistic and structural details are still under discussion.

A considerable number of diferrous and diferric model complexes for these enzymes have been synthesized and spectroscopically and structurally characterized using a variety of ligand systems. Detailed overviews of characterized diiron model complexes can be found in the literature.[14−21] Several ligand systems have been employed to form diiron(III) peroxo complexes, and the structures of the three dinuclear peroxo bridged iron compounds $[Fe_2(O_2)(C_6H_5CH_2COO)_2\{(HB(pz')_3\}_2]$, $[Fe_2(N\text{-}Et\text{-}HPTB)(O_2)(Ph_3PO)_2](BF_4)_3\cdot 3CH_3CN$, and $[Fe_2(Ph\text{-}bimp)(O_2)(C_6H_5COO)](BF_4)_2\cdot 2CH_3CN\cdot C_2H_5OC_2H_5\cdot H_2O$ have been published recently.[22−25] They were prepared by the reaction of the corresponding diferrous precursor complex with dioxygen.

‡ Dedicated to Professor Heinrich Vahrenkamp on the occasion of his 60th birthday.

§ Fax: (+49)-251-8338366. E-mail: krebs@uni-muenster.de.

|| Fax: (+49)-9131-8527387. E-mail: schindls@anorganik.chemie.uni-erlangen.de.

(1) Holmes, M. A.; Le Trong, I.; Turley, S.; Sieker, L. C.; Stenkamp, R. E. *J. Mol. Biol.* **1991**, *218*, 583−593.
(2) Nordlund, P.; Sjöberg, B.-M.; Eklund, H. *Nature* **1990**, *345*, 593−598.
(3) Rosenzweig, A. C.; Frederick, C. A.; Lippard, S. J.; Nordlund, P. *Nature* **1993**, *366*, 537−543.
(4) Sträter, N.; Klabunde, T.; Tucker, P.; Witzel, H.; Krebs, B. *Science* **1995**, *268*, 1489−1492.
(5) Sträter, N.; Lipscomb, W. N.; Klabunde, T.; Krebs, B. *Angew. Chem., Int. Ed. Engl.* **1996**, *35*, 2024−2057.
(6) Klabunde, T.; Krebs, B. *Struct. Bonding* **1997**, *89*, 177−198.
(7) Uppenberg, J.; Lindqvist, F.; Svensson, C.; Ek-Rylander, B.; Andersson, G. *J. Mol. Biol.* **1999**, *290*, 201−211.
(8) Lindquist, Y.; Johannson, E.; Kaija, H.; Vihko, P.; Schneider, G. *J. Mol. Biol.* **1999**, *291*, 135−147.
(9) Guddat, L. W.; McAlpine, A. S.; Hume, D.; Hamilton, S.; deJersey, J.; Marin, J. L. *Structure* **1999**, *7*, 757−767.
(10) Reedijk, J. *Bioinorganic Catalysis*; Marcel Dekker: New York, 1999.
(11) Wallar, B. J.; Lipscomb, J. D. *Chem. Rev.* **1996**, *96*, 2625−2657.
(12) Lange, S. J.; Que, L., Jr. *Curr. Opin. Chem. Biol.* **1998**, *2*, 159−172.
(13) Suerbaum, H.; Körner, M.; Witzel, H.; Althaus, E.; Mosel, B. M.; Müller-Warmuth, W. *Eur. J. Biochem.* **1993**, *214*, 313−321.
(14) Lippard, S. J. *Angew. Chem., Int. Ed. Engl.* **1988**, *27*, 344−361.
(15) Sanders-Loehr, J.; Wheeler, W. D.; Schiemke, A. K.; Averill, B. A.; Loehr, T. M. *J. Am. Chem. Soc.* **1989**, *111*, 8084−8093.
(16) Kurtz, D. M., Jr. *Chem. Rev.* **1990**, *90*, 585−606.
(17) Vincent, J. B.; Lilley, G. C.; Averill, B. A. *Chem. Rev.* **1990**, *90*, 1447−1467.
(18) Que, L., Jr.; True, A. E. *Prog. Inorg. Chem.* **1990**, *38*, 97−200.
(19) Fontecave, M.; Ménage, S.; Duboc-Toia, C. *Coord. Chem. Rev.* **1998**, *178*−*180*, 1555−1572.
(20) Westerheide, L.; Pascaly, M.; Krebs, B. *Curr. Opin. Chem. Biol.* **2000**, *4*, 235−241.
(21) Girerd, J.-J.; Banse, F.; Simaan, A. J. In *Characterization and Properties of Non-Heme Iron Peroxo Complexes*; Meunier, B., Ed.; Springer-Verlag: Berlin, Heidelberg, 2000; Vol. 97, pp 146−177.

10.1021/ic0009371 CCC: $20.00 
Published on Web 03/15/2001

**Scheme 1**

| general structure type | substituents | ref. |
|---|---|---|
| 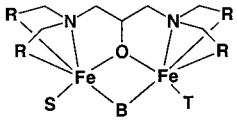 | R = Bzim; S, T = $NO_3$; B = $\mu$-OH (**1**)<br>R = Bzim; S, T = OBz; B = $\mu$-OH (**3**)<br>R = Bzim; S, T = $NO_3$; B = $\mu$-$OCH_3$ (**2**)<br>R = Bzim; S = Cl; T = $H_2O$; B = $\mu$-$O_2As(CH_3)_2$<br>R = Bzim; S = $OCH_3$; T = $HOCH_3$; B = $\mu$-$O_2As(CH_3)_2$<br>R = Bzim; S, T = $P(C_6H_5)_3$; B = $\mu$-O-O<br>R = N-Et-Bzim; S, T = $NO_3$; B = $\mu$-OH<br>R = N-EtOH-Bzim; S, T = $NO_3$; B = $\mu$-OH (**4**)<br>R = 5,6-$Me_2$Bzim; S, T = $NO_3$; B = $\mu$-OH (**5**) | [28, 50]<br><br><br>[37]<br>[40]<br><br>[25]<br>[47]<br><br><br> |
| 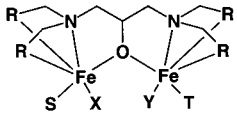 | R = Bzim; S = $O_2P(OC_6H_5)$; T = $HOCH_3$; X, Y = Cl | [62] |
| 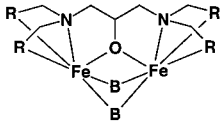 | R = Bzim; B = $\mu$-$O_3P$(OH) | [57] |

| residue R | abbreviation | residue R | abbreviation | residue R | abbreviation | residue R | abbreviation |
|---|---|---|---|---|---|---|---|
| 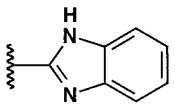 | Bzim | 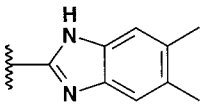 | 5,6-$Me_2$-Bzim | 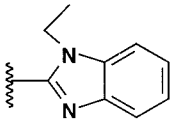 | N-Et-Bzim | 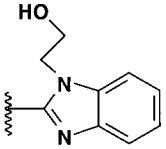 | N-EtOH-Bzim |

| general structure type | substituents | ref. |
|---|---|---|
| 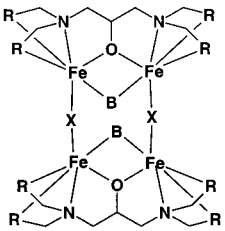 | R = Bzim; B = $\mu$-OBz; X = $\mu$-O<br>R = N-Et-Bzim; B = $\mu$-OAc; $\mu$-O | [52]<br>[52] |
| 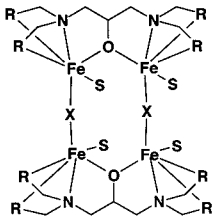 | R = Bzim; S = OH; X = $\mu$-F (**6**) | |
| 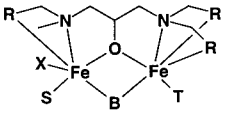 | R = Bzim; S, T = Cl; B = $\mu$-$O_2As(CH_3)$; X = $HOCH_3$ | [38] |

In all of these complexes a $\mu$-1,2 binding mode of the peroxo ligand is observed.

The reaction of the dinuclear iron(II) complex $[Fe_2$(N-Et-HPTB)(OBz)$]^{2+}$ with dioxygen was studied in more detail, and two mechanisms for the formation and decay of the peroxo complex were postulated.[25,26] It was recognized that the structure of the ligand backbone as well as the nature of additional bridging ligands plays an important role for the stability of the resulting peroxo complexes.[27] Furthermore, it was discovered that the solvent can dramatically alter the stability of the iron peroxo species, but the intricate details of these effects remained unclear.[27,28]

Another strategy for synthesizing diiron(III) peroxo species is adding hydrogen peroxide to diferric precursor complexes. The (1:1) peroxide adduct of $[Fe_2$(HPTB)($\mu$-OH)$(NO_3)_2](NO_3)_2$ (**1**) has been reported previously, but no X-ray structure was determined.[29] The spectroscopic, magnetic, and electrochemical investigations suggest a $\mu$-1,2-coordination of the peroxide.[28]

Our own interest in this field of research is focused on the investigation of PAPs and their model complexes as well as on their use for the analytical detection of hydrogen peroxide.[30−34] Recently, "peroxidase-like" activity has been observed for the mammalian PAPs and a function as an oxygen activator is discussed for these enzymes.[13,35] For that reason we have studied a large number of dinuclear iron(III) complexes with HPTB[36] and its derivatives as ligands in combination with different additional ligands, bridging and nonbridging.[30−34,37−39] All structurally characterized iron(III) complexes known of this type are presented in Scheme 1.

Recently we have begun to investigate the mechanism of the reaction of hydrogen peroxide with these complexes varying

(22) Abbrevations of ligands used: $HB(pz')_3$ = hydrotis(3,5-diisopropyl-1-pyrazol)borate; N-Et-HPTB = *N*,*N*,*N*′,*N*′-tetrakis(*N*-ethyl-2-benzimidazolylmethyl)-2-hydroxo-1,3-diaminopropane; Ph-bimp = 2,6-bis{bis[2-(1-methyl-4,5-diphenylimidazolyl)methyl]aminomethyl}-4-methylphenolate.

(23) Kim, K.; Lippard, S. J. *J. Am. Chem. Soc.* **1996**, *118*, 4914−4915.
(24) Ookubo, T.; Sugimoto, H.; Nagayama, T.; Masuda, H.; Sato, T.; Tanaka, K.; Maeda, Y.; Okawa, H.; Hayashi, Y.; Uehara, A.; Suzuki, M. *J. Am. Chem. Soc.* **1996**, *118*, 701−702.
(25) Dong, Y. H.; Yan, S. P.; Young, V. G.; Que, L., Jr. *Angew. Chem., Int. Ed. Engl.* **1996**, *35*, 618−620.
(26) Feig, A. L.; Becker, M.; Schindler, S.; van Eldik, R.; Lippard, S. J. *Inorg. Chem.* **1996**, *35*, 2590−2601.
(27) Dong, Y.; Ménage, S.; Brennan, B. A.; Elgren, T. E.; Jang, H. G.; Pearce, L. L.; Que, L., Jr. *J. Am. Chem. Soc.* **1993**, *115*, 1851−1859.
(28) Brennan, B.; Chen, Q.; Juarez-Garcia, C.; True, A.; O'Connor, C.; Que, L., Jr. *Inorg. Chem.* **1991**, *30*, 1937−1943.
(29) Nishida, Y.; Takeuchi, M.; Shimo, H.; Kida, S. *Inorg. Chim. Acta* **1984**, *96*, 115−119.
(30) Krebs, B.; Ahlers, F.; Bremer, B.; Eulering, B.; Klabunde, T.; Schepers, K.; Schmidt, M.; Sträter, N.; Than, R.; Witzel, H. In *Bioinorganic Chemistry*; Trautwein, A. X., Ed.; VCH: Weinheim, 1997; pp 412−425.
(31) Witzel, H.; Krebs, B.; Bruch, A.; Büldt-Karentzopoulos, K.; Dietrich, M.; Durmus, A.; Eicken, C.; Fischer, H.; Klabunde, T.; Körner, M.; Meiwes, D.; Münstermann, D.; Löcke, R.; Rompel, A.; Stahl, B.; Sträter, N.; Suerbaum, H. In *Bioinorganic Chemistry*; Trautwein, A. X., Ed.; VCH: Weinheim, 1997; pp 385−396.
(32) Than, R.; Feldmann, A. A.; Krebs, B. *Coord. Chem. Rev.* **1999**, *182*, 211−241.
(33) Harms, D.; Than, R.; Pinkernell, U.; Schmidt, M.; Krebs, B.; Karst, U. *Analyst* **1998**, *123*, 2323.
(34) Harms, D.; Meyer, J.; Westerheide, L.; Krebs, B.; Karst, U. *Anal. Chim. Acta* **1999**, *19980*, 1−8.
(35) Hayman, A. R.; Cox, T. M. *J. Biol. Chem.* **1994**, *269*, 1294−1300.
(36) HPTB = *N*,*N*,*N*′,*N*′-tetrakis(2-benzimidazolylmethyl)-2-hydroxo-1,3-diaminopropane; the abbrevation Htbpo is used as well.
(37) Eulering, B.; Ahlers, F.; Zippel, F.; Schmidt, M.; Nolting, H.-F.; Krebs, B. *J. Chem. Soc., Chem. Commun.* **1995**, 1305−1307.
(38) Eulering, B.; Schmidt, M.; Pinkernell, U.; Karst, U.; Krebs, B. *Angew. Chem., Int. Ed. Engl.* **1996**, *35*, 1973−1974.

the conditions and parameters: concentration, temperature, pressure, and the additional ligands.[40] We have now extended this work by modifying the ligand backbone and by the systematic variation of the solvent to gain a more fundamental understanding of the formation, stabilization, and properties of dinuclear iron peroxo complexes. Accordingly, the new complexes **2**−**6** (Scheme 1) were synthesized and structurally characterized and their reaction with hydrogen peroxide in different solvents was investigated.

## Experimental Section

**General Remarks.** All chemicals were purchased commercially and used as received. Chemicals of analytical reagent grade and ultrapure water were used throughout this study. **CAUTION!** The perchlorate salts used in this study are potentially explosive and should be handled with care.

**Physical Measurements.** $^1$H NMR spectra were recorded on a Bruker WH 300 instrument; all chemical shifts are reported relative to an internal standard of tetramethylsilane. $^{19}$F NMR spectra were recorded on a Bruker AC 200 instrument using trichlorofluoromethane as external standard. Elemental analyses were performed on a Heraeus CHN-O-RAPID instrument. Conductivity measurements were performed with a WTW LF 9020 (WTW, Wiss. Techn. Werkst., Weilheim, Germany), and solutions of KCl, $BaCl_2$, and $K_3[Fe(CN)_6]$ were used in comparison as 1:1, 1:2, and 1:3 electrolyte.

Kinetic studies of the reactions of hydrogen peroxide with iron(III) complexes were recorded on a modified Hi Tech SF-3L low-temperature stopped-flow unit (Salisbury, U.K.) equipped with a J&M TIDAS 16-500 diode array spectrophotometer (J&M, Aalen, Germany). The kinetic data were treated by a global analysis fitting routine using the program Specfit (Spectrum Software Associates, Chapel Hill) and/or by extracting single absorbance vs time traces at different wavelengths. These traces were fitted to single-exponential functions using the integrated J&M software Kinspec. Complex solutions were $1 \times 10^{-4}$ M, and the concentration of the hydrogen peroxide solutions was varied from $1 \times 10^{-3}$ to $1 \times 10^{-2}$ M. Hydrogen peroxide solutions were prepared by adding hydrogen peroxide (30%, titrated with $KMnO_4$) with micropipets to the solution (the amount of water was kept constant by adding small amounts of water as well).

***N,N,N′,N′*-Tetrakis(2-benzimidazolylmethyl)-2-hydroxo-1,3-diaminopropane (HPTB).** A higher purity of the product was achieved by avoiding the preparation of the hydrochloride intermediate.[37] 1,3-Diamino-2-propanol-*N,N,N′,N′*-tetraacetic acid (12.9 g, 0.0375 mol) and 1,2-diaminobenzene (16.22 g, 0.15 mol) were ground to a fine powder and mixed thoroughly. The mixture was heated to 180 °C for 2 h until all the water was evaporated. The resulting red glass was dissolved in ethanol and refluxed with activated charcoal for 30 min. Filtration and evaporation yielded a pale brown residue. The product precipitated as a white powder upon the addition of water to a solution of the crude product in acetone. Yield: 17.17 g (0.028 mol, 74%), mp 169 °C. Anal. Calcd for $C_{35}H_{34}N_{10}O$: C, 68.83; H, 5.61; N, 22.93. Found: C, 68.57; H, 5.45; N, 22.70. $^1$H NMR (300 MHz, DMSO-$d_6$, TMS): $\delta$ [ppm] 2.50 (m, 4H), 2.68 (m, 1H), 4.04 (s, 8H), 6.43 (s, 1H), 7.18 (m, 8H), 7.51 (m, 8H).

***o*-Nitro-*N*-(2-hydroxoethyl)aniline.** This compound was synthesized according to a procedure described by McManus et al.[41] To a solution of 6.875 g (0.06 mol) of *o*-nitrobromobenzene in 47.5 mL (0.79 mol) of ethanolamine was added 1.125 g of anhydrous cupric chloride. The resulting mixture was heated for 90 min taking care that the temperature did not rise above 90 °C. The reaction mixture was then poured into ice and water. Filtration and drying of the precipitating solid gave a red colored product. Yield: 9.6 g (53 mmol, 89%), mp 73 °C. Anal. Calcd for $C_8H_{10}N_2O_3$: C, 52.74; H, 5.53; N, 15.38. Found: C, 52.50; H, 5.61; N, 15.03. $^1$H NMR (300 MHz, $CDCl_3$, TMS): $\delta$ [ppm] 1.96 (s, 1H), 3.51 (dt, 2H), 3.94 (t, 2H), 6.65 (m, 1H), 6.89 (dd, 1H), 7.44 (m, 1H), 8.16 (dd, 1H), 8.24 (t, 1H).

***o*-Amino-*N*-(2-hydroxoethyl)aniline.** This compound was prepared by the slight modification of the procedure described by Ramage and Trappe.[42] A solution of 1.6 g (50 mmol) of sulfur and 12.0 g (153.8 mmol) of sodium sulfide in 50 mL of water was refluxed for 2 h with 4.55 g (25 mmol) of *o*-nitro-*N*-(2-hydroxoethyl)aniline. Upon cooling, the product crystallized as colorless plates. Yield: 3.3 g (21.7 mmol, 87%), mp 105 °C. Anal. Calcd for $C_8H_{12}N_2O$: C, 63.14; H, 7.9; N, 18.41. Found: C, 62.98; H, 8.05; N, 18.16. $^1$H NMR (300 MHz, $CDCl_3$, TMS): $\delta$ [ppm] 3.25 (t, 2H), 3.79 (dt, 2H), 4.49 (t, 1H), 4.57 (s, 2H), 4.83 (t, 1H), 6.57−6.75 (m, 4H).

***N,N,N′,N′*-Tetrakis(*N″*-(2-hydroxoethyl)-2-benzimidazolylmethyl)-2-hydroxo-1,3-diaminopropane (N-EtOH-HPTB).** The polypodal ligand N-EtOH-HPTB was synthesized according to the general procedure described for the ligand HPTB. A mixture of 6.08 g (0.04 mol) of *o*-amino-*N*-(2-hydroxoethyl)aniline and 4.23 g (0.01 mol) of the perchloric acid adduct of 1,3-diamino-2-propanol-*N,N,N′,N′*-tetraacetic acid was heated to 180 °C for 2 h until all water was evaporated. The glassy residue was dissolved in ethanol and refluxed for 30 min. Active charcoal was added, and after 15 min the hot solution was filtered. Upon cooling the crude product precipitated and was filtered off. Recrystallization from ethanol gave a white powder, which is the perchloric acid adduct of the ligand N-EtOH-HPTB. Yield: 4.95 g (0.0056 mol, 56%), mp 135 °C. Anal. Calcd for $C_{43}H_{50}N_{10}O_5 \cdot HClO_4$: C, 58.20; H, 5.68; N, 15.78. Found: C, 58.05; H, 5.84; N, 15.68. $^1$H NMR (300 MHz, DMSO-$d_6$, TMS): $\delta$ [ppm] 2.50−2.70 (m, 4H), 3.38 (m, 1H), 3.70−3.95 (m, 8H), 4.05 (m, 8H), 4.14 (m, 8H), 7.16 (m, 8H), 7.53 (m, 8H).

***N,N,N′,N′*-Tetrakis(5,6-dimethyl-2-benzimidazolylmethyl)-2-hydroxo-1,3-diaminopropane (5,6-Me$_2$-HPTB).** The heptadentate ligand 5,6-Me$_2$-HPTB was synthesized in a manner similar to the procedure described for the ligand HPTB. A mixture of 5.46 g (0.04 mol) of 4,5-dimethyl-2-aminoaniline and 4.23 g (0.01 mol) of the perchloric acid adduct of 1,3-diamino-2-propanol-*N,N,N′,N′*-tetraacetic acid was heated to 180 °C for 2 h until all the water was evaporated. The glassy residue was dissolved in ethanol and refluxed for 1 h. Active charcoal was added, and after 15 min the hot solution was filtered. Upon cooling the crude product precipitated and was filtered off. Recrystallization from ethanol yielded a gray-white powder, which was characterized as the perchloric acid adduct of the ligand 5,6-Me$_2$-HPTB. Yield: 4.36 g (0.0053 mol, 53%), mp 181 °C. Anal. Calcd for $C_{43}H_{50}N_{10}O \cdot HClO_4$: C, 62.27; H, 6.24; N, 17.01. Found: C, 61.99; H, 6.54; N, 16.78. $^1$H NMR (300 MHz, DMSO-$d_6$, TMS): $\delta$ [ppm] 2.32 (s, 24H), 2.59 (dd, 2H), 2.80 (dd, 2H), 3.98 (m, 1H), 4.11 (s, 8H), 7.26 (s, 8H).

**[Fe$_2$(HPTB)($\mu$-OH)(NO$_3$)$_2$](NO$_3$)$_2$·CH$_3$OH·2H$_2$O (1).** This compound was synthesized according to the procedure reported by Que et al.[28] The ligand HPTB (0.122 g, 0.2 mmol) was dissolved in 20 mL of methanol; 0.2 g (0.4 mmol) of $Fe(NO_3)_3 \cdot 9H_2O$ was added. Upon standing at room temperature, the dark orange solution yielded a red microcrystalline powder. Yield: 0.097 g (0.092 mmol, 46%). Anal. Calcd for $C_{36}H_{42}Fe_2N_{14}O_{17}$: C, 41.04; H, 3.92; N, 18.61. Found: C, 41.01; H, 3.84; N, 18.38.

**[Fe$_2$(HPTB)($\mu$-OCH$_3$)(NO$_3$)$_2$](NO$_3$)$_2$·4.5CH$_3$OH (2).** Triethylamine (50 $\mu$L) was added to a solution of 0.122 g (0.2 mmol) of the ligand HPTB and 0.2 g (0.4 mmol) of $Fe(NO_3)_3 \cdot 9H_2O$ in 18 mL of methanol, changing the color of the solution from red to dark red. Upon standing for 1 day at room temperature red needlelike crystals were obtained. Yield: 0.12 g (0.105 mmol, 52.5%). Anal. Calcd for $C_{40.5}H_{54}Fe_2N_{14}O_{18.5}$: C, 42.50; H, 4.76; N, 17.13. Found: C, 42.34; H, 4.98; N, 17.32.

**[Fe$_2$(HPTB)($\mu$-OH)(OBz)$_2$](ClO$_4$)$_2$·4.5H$_2$O (3).** A solution of 0.122 g (0.2 mmol) of the ligand HPTB in 5 mL of methanol was added to 2.5 mL of an aqueous solution of $Fe(ClO_4)_3 \cdot 9H_2O$ (0.207 g, 0.4 mmol) and sodium benzoate (0.029 g, 0.2 mmol), resulting in a deep red mixture. After standing for several months at room temperature red

(39) Krebs, B.; Büldt-Karentzopoulos, K.; Eicken, C.; Rompel, A.; Witzel, H.; Feldmann, A.; Kruth, R.; Reim, J.; Steinforth, W.; Teipel, S.; Zippel, F.; Schindler, S.; Wiesemann, F. In *Catechol oxidase: model compounds and structure of the active site*; Trautwein, A. X., Ed.; VCH: Weinheim, 1997; p 616.

(40) Than, R.; Schrodt, A.; Westerheide, L.; van Eldik, R.; Krebs, B. *Eur. J. Inorg. Chem.* **1999**, 1537−1543.

(41) McManus, J. M.; Herbst, R. M. *J. Org. Chem.* **1959**, *24*, 1042−1044.

(42) Ramage, G. R.; Trappe, G. *J. Chem. Soc.* **1952**, 4406−4409.

**Table 1.** Selected Crystallographic Data[a]

| compd | **2** | **3** | **4** | **5** | **6** |
|---|---|---|---|---|---|
| formula | $C_{36}H_{36}Fe_2N_{14}O_{14}\cdot 4.5MeOH$ | $C_{49}H_{44}Cl_2Fe_2N_{10}O_{14}\cdot 4.5H_2O$ | $C_{43}H_{50}ClFe_2N_{13}O_{19}\cdot 3MeOH\cdot 1.5H_2O$ | $C_{43}H_{50}ClFe_2N_{13}O_{15}\cdot 3.5MeOH\cdot Et_2O\cdot 0.5H_2O$ | $C_{70}H_{70}Cl_4F_2Fe_4N_{20}O_{22}\cdot MeCN\cdot Et_2O\cdot H_2O$ |
| fw (g/mol) | 1144.68 | 1260.64 | 1323.27 | 1331.40 | 2079.87 |
| cryst syst | triclinic | orthorhombic | triclinic | triclinic | triclinic |
| space group | $P\bar{1}$ | $Pca2_1$ | $P\bar{1}$ | $P\bar{1}$ | $P\bar{1}$ |
| $a$ (Å) | 12.435(2) | 23.171(5) | 14.768(3) | 11.367(3) | 14.620(3) |
| $b$ (Å) | 15.383(3) | 20.686(4) | 15.249(3) | 16.107(3) | 14.851(3) |
| $c$ (Å) | 16.053(3) | 23.590(5) | 16.264(3) | 20.197(3) | 22.141(3) |
| α (deg) | 65.95(3) | 90 | 69.69(3) | 70.27(3) | 84.49(3) |
| $\beta$ (deg) | 72.08(3) | 90 | 70.56(3) | 76.70(3) | 79.66(3) |
| $\gamma$ (deg) | 74.22(3) | 90 | 70.26(3) | 70.57(3) | 88.32(3) |
| $V$ (Å$^3$) | 2629.91 | 11307.05 | 3135.14 | 3253.51 | 4707.01 |
| $Z$ | 2 | 8 | 2 | 2 | 2 |
| $\rho$(calcd) (g/cm$^3$) | 1.446 | 1.469 | 1.390 | 1.357 | 1.465 |
| temp (K) | 213 | 213 | 213 | 213 | 170 |
| $\theta_{range}$ (deg) | 4.3−25.9 | 4.3−26.1 | 4.4−26.1 | 4.4−25.9 | 2.0−27.0 |
| measd reflns | 20634 | 88674 | 24935 | 25526 | 20911 |
| indep reflns | 9449 | 21527 | 11369 | 11747 | 20135 |
| $R_{int}$ (%) | 11.48 | 14.00 | 10.54 | 8.54 | 4.39 |
| obsd reflns [$I > 2\sigma(I)$] | 5685 | 16501 | 7617 | 8069 | 9235 |
| params | 690 | 1469 | 823 | 796 | 1183 |
| R1; wR2 (%) [$I > 2\sigma(I)$] | 7.25; 16.17 | 6.32; 15.05 | 6.77; 17.98 | 6.34; 15.32 | 7.37; 20.03 |

[a] Mo Kα radiation ($\lambda = 0.71073$ Å).

crystals suitable for X-ray characterization were obtained. Yield: 0.013 g (0.01 mmol, 5%). Anal. Calcd for $C_{49}H_{53}Cl_2Fe_2N_{10}O_{18.5}$: C, 46.68; H, 4.23; N, 11.11. Found: C, 47.01; H, 4.14; N, 11.38.

**[$Fe_2$(N-EtOH-HPTB)($\mu$-OH)($NO_3$)$_2$]($ClO_4$)($NO_3$)·3$CH_3OH$·1.5$H_2O$ (4).** A solution of N-EtOH-HPTB·$HClO_4$ (0.1 g, 0.113 mmol) in 15 mL of methanol was treated with a solution of $Fe(NO_3)_3\cdot 9H_2O$ (0.091 g, 0.226 mmol) in 15 mL of methanol. Upon standing, a red-orange microcrystalline powder of **4** precipitated and was filtered off. Single crystals of **4** suitable for X-ray characterization were obtained by vapor diffusion of diethyl ether into a methanol/*n*-butanol solution of **4**. Yield: 0.055 g (0.042 mmol, 37%). Anal. Calcd for $C_{46}H_{65}ClFe_2N_{13}O_{23.5}$: C, 41.75; H, 4.95; N, 14.82. Found: C, 42.08; H, 5.11; N, 14.09.

**[$Fe_2$(5,6-$Me_2$-HPTB)($\mu$-OH)($NO_3$)$_2$]($ClO_4$)($NO_3$)·3.5$CH_3OH$·$C_2H_5OC_2H_5$·0.5$H_2O$ (5).** By vapor diffusion of 40 mL of diethyl ether to a solution of 5,6-$Me_2$-HPTB·$HClO_4$ (0.082 g, 0.1 mmol) and $Fe(NO_3)_3\cdot 9H_2O$ (0.081 g, 0.2 mmol) in 40 mL of methanol red needlelike crystals of **5** precipitated. Yield: 0.038 g (0.028 mmol, 28%). Anal. Calcd for $C_{50.5}H_{75}ClFe_2N_{13}O_{20}$: C, 45.56; H, 5.68; N, 13.68. Found: C, 45.11; H, 5.16; N, 13.45.

**[$Fe_4$(HPTB)$_2$($\mu$-F)$_2$(OH)$_4$]($ClO_4$)$_4$·$CH_3CN$·$C_2H_5OC_2H_5$·$H_2O$ (6).** The ligand HPTB (0.1 g, 0.164 mmol), $Fe(ClO_4)_3\cdot 9H_2O$ (0.17 g, 0.328 mmol), pyrazole (0.023 g, 0.328 mmol), and $NaBF_4$ (0.036 g, 0.328 mmol) were dissolved in 150 mL of acetonitrile. Upon stirring the orange solution, a small amount of effervescence was observed. By vapor diffusion of 10 mL diethyl ether to 10 mL of the solution orange crystals of **6** were obtained after several days. Yield: 0.059 g (0.028 mmol, 17%). Anal. Calcd for $C_{76}H_{85}Cl_4F_2Fe_4N_{21}O_{24}$: C, 43.89; H, 4.12; N, 14.14. Found: C, 44.04; H, 4.36; N, 13.98. $^{19}$F NMR (200 MHz, $CD_3CN$): $\delta$ [ppm] 141.2 (s, br).

**Single-Crystal X-ray Structure Determinations.** The crystallographic data of **2**−**5** were collected on a STOE IPDS diffractometer (Mo Kα, $\lambda = 0.71073$ Å, graphite monochromator) with a sample-to-plate distance of 70 mm and a scan range from 0° to 180° with an exposure time of 4 min per 0.8° increment for **2**, 8.5 min per 0.7° increment for **3**, 3.5 min per 1.2° increment for **4**, and 3 min per 1.0° increment for **5**. A combined absorption and decay correction was applied.[43] Intensity data for complex **6** were collected on a Siemens P3 four-circle diffractometer (Mo Kα, $\lambda = 0.71073$ Å, graphite monochromator) using the $\omega$-scan method. The intensities of two reflections were monitored, and no significant crystal deterioration was observed. Further data collection parameters are summarized in Table 1. The structures were solved by Patterson methods.[44] A series of full-matrix least-squares refinement cycles on $F^2$, followed by Fourier syntheses, gave the location of all remaining atoms.[45] The hydrogen atoms were placed at calculated geometric positions and were constrained to ride on the parent atom to which they were attached. The isotropic thermal parameters for the methyl and hydroxyl protons were refined with 1.5 times the $U_{eq}$ value of the corresponding atom and for all other hydrogen atoms with 1.2 $U_{eq}$. The non-hydrogen atoms were refined with anisotropic thermal parameters with the exception of all solvent molecules in **6** ($CH_3CN$, $C_2H_5OC_2H_5$, $H_2O$), which were severely disordered.

## Results and Discussion

To model the chemistry of dinuclear iron proteins, as for example MMO, different low molecular weight iron(II) complexes were synthesized to study the reversible dioxygen uptake of such molecules. The use of dinucleating ligands which utilize a 2-hydroxypropane unit to link two tridentate $N_3$ ligands proved to be a successful approach for these investigations.[21,26,27,46] For example, the reaction of [$Fe_2$(N-Et-HPTB)(OBz)]$^{2+}$ with dioxygen at low temperatures allowed the isolation and structural characterization of one of the few iron peroxo complexes known up till now.[25] A kinetic study revealed that this peroxo complex is very labile at room temperature and decomposes irreversibly after a few seconds.[26] Interestingly, the same peroxo complex can be prepared by mixing hydrogen peroxide with the dinuclear iron(III) complex. But in this case the dioxygen adduct had a much higher stability. Depending on the conditions the peroxo complex could be observed for several hours at room temperature. Especially remarkable was the influence of solvent, an effect which had been observed for the reaction of the iron(II) complex with dioxygen as well.[25,27] To gain better insight into

(43) Program DECAY [STOE IPDS software package, STOE & CIE, Darmstadt, 1993].

(44) Program XS [Sheldrick, G. M. *SHELXTL PLUS*; Siemens Analytical X-ray Instruments: Madison, WI, 1990].

(45) Program SHELXL 97 [Sheldrick, G. M. *SHELXL 97, Program for Crystal Structure Determinations*; University of Göttingen: Göttingen, Germany, 1997].

(46) Que, L., Jr. *J. Chem. Soc., Dalton Trans.* **1997**, 3933−3940.

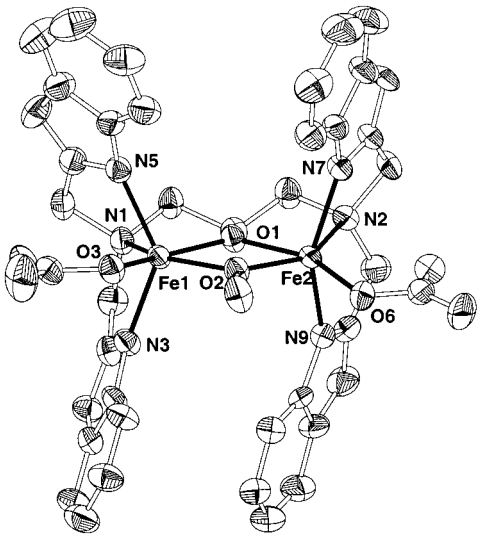


**Figure 1.** Structure of the cation in **2** showing 50% probability ellipsoids; hydrogen atoms have been omitted for clarity.

these effects we decided to study the reaction of hydrogen peroxide with a series of iron(III) complexes in different solvents. The ligands we used can be regarded as derivatives of the parent ligand HPTB.[36] This ligand was modified mainly to increase the solubility of the dinculear iron(III) complexes in different solvents.

The iron(III) complex $[Fe_2(HPTB)(\mu\text{-}OH)(NO_3)_2](NO_3)_2{\cdot}CH_3OH{\cdot}2H_2O$ (**1**) was prepared and crystallized as the nitrate salt. The crystal structures of $[Fe_2(HPTB)(\mu\text{-}OH)(NO_3)_2]^{2+}$ and of the related compound $[Fe_2(N\text{-}Et\text{-}HPTB)(\mu\text{-}OH)(NO_3)_2]^{2+}$ have been reported previously.[28,29,47] In both cases disorder problems were observed during the crystal structure refinement procedure. To study the effect of different bridging groups the hydroxo group in **1** has been successfully replaced by other anions by us and other groups as shown in Scheme 1.

Upon adding $NEt_3$ to a methanolic solution of **1** the color turned from orange to deep red and crystals formed soon afterward. The crystal structure analysis revealed that the methoxo-bridged analogue of **1** was formed. An ORTEP plot of the cation in $[Fe_2(HPTB)(\mu\text{-}OCH_3)(NO_3)_2](NO_3)_2{\cdot}4.5CH_3OH$ (**2**) is shown in Figure 1. Structural details are given in Table 2.

In **2**, the two iron centers are bridged by one alkoxo oxygen atom (O(1) of HPTB) and a $\mu$-methanolato ligand. The substitution of $OH^-$ in **1** by $OCH_3^-$ in **2** does not cause any significant structural changes. The metal−metal separation in **2** [3.239(1) Å] is slightly longer than in **1** [3.177(3) Å] as the methanolato ligand is more bulky than the hydroxo group. Interestingly, in compound **2** the $N_{amine}-Fe-O_{NO_3}$ angles are enlarged and the terminally ligated nitrates are asymmetrically chelated. Similar structural features were described for the analogous complex $[Fe_2(DBE)_2(NO_3)_2](NO_3)_2$ (DBE = 2-[2-bis(2-benzimidazolylmethyl)amino]ethanol).[48] This compound also contains an $Fe_2(OR)_2$ core, elongated $Fe-N_{amine}$ bonds [2.311(8) Å], and enlarged $N_{amine}-Fe-O_{NO_3}$ angles to allow asymmetric coordination of the nitrate ligands [2.067(10) and 2.682(10) Å].

Benzoate is a useful ligand to model the carboxylate-bridged non-heme diiron active sites.[49] We tried to use this ligand as well to substitute the hydroxo bridge in **1**. Earlier attempts by other groups to synthesize this complex were unsuccessful, and only the hydroxo-bridged compound similar to **1** was obtained instead. This was explained by the facile replacement of the benzoate group by nitrate ions.[50] In contrast to these earlier findings we were able to obtain crystals suitable for structural characterization from an aqueous methanol solution of the ligand HPTB, sodium benzoate, and $Fe(ClO_4)_3{\cdot}9H_2O$, avoiding the use of nitrate as counterion. The crystals turned out to be $[Fe_2(HPTB)(\mu\text{-}OH)(OBz)_2](ClO_4)_2{\cdot}4.5H_2O$ (**3**). The structural data are given in Table 2. The structure of **3** contains two slightly different $[Fe_2(HPTB)(\mu\text{-}OH)(OBz)_2]^{2+}$ cations in the asymmetric unit. As an example one of the two cations is shown in Figure S1 (Supporting Information). The two iron centers have distorted octahedral coordination in each of the cations (**3a** and **3b**). The iron centers are bridged by the alkoxo oxygen atom O(1) of the ligand HPTB and a hydroxo group. The octahedral coordination sphere of both iron atoms is completed by three nitrogen atoms of the HPTB ligand and one oxygen atom of the benzoate group. Additionally, four perchlorate anions and nine water solvent molecules are present in the asymmetric unit.

In both cations **3a** and **3b**, the $Fe-O_{OBz}$ bond lengths [Fe(1)−O(3), Fe(1a)−O(3a), Fe(2)−O(5), Fe(2a)−O(5a)] are between 1.981(4) and 2.003(5) Å, which is in the expected range of iron(III) carboxylate interactions.[51] The benzoate groups in **3** are not bridging the iron atoms in a bidentate mode as was found in a series of related diiron(III) complexes and was suggested earlier for **3**.[52] Instead, they are terminally coordinated to the iron ions with weak secondary interactions via the second carbonyl oxygen atoms resulting in a chelated coordination of one benzoate ligand at each iron center. The essential features of the structure of **3** are similar to the analogous dinuclear iron(III) complex $[Fe_2(DBE)_2(OBz)_2](ClO_4)_2$ described earlier.[53] In this compound, a separation of 3.21(1) Å was observed for a bis($\mu$-alkoxo) bridged diiron(III) unit, compared to 3.219(1) Å on average in **3** for the ($\mu$-alkoxo)($\mu$-hydroxo) bridged diiron(III) core. In both complexes, the benzoate ligands are coordinated in a monodentate fashion to the iron centers with average $Fe-O_{OBz}$ distances of 1.994 Å in **3** and 1.99 Å in $[Fe_2(DBE)_2(OBz)_2](ClO_4)_2$ and show weak secondary interactions between the carbonyl oxygen atoms and the iron ions.

All compounds reported so far (**1**−**3**) are not very soluble in aqueous and organic solvents. To improve the solubility of the ligand and the resulting diiron complexes in water we introduced additional alcohol groups into the ligand backbone. Accordingly, the new ligand N-EtOH-HPTB was synthesized and reacted with iron(III) nitrate to give $[Fe_2(N\text{-}EtOH\text{-}HPTB)(\mu\text{-}OH)(NO_3)_2](ClO_4)(NO_3){\cdot}3CH_3OH{\cdot}1.5H_2O$ (**4**). Crystals suitable for X-ray structural characterization were obtained, and an ORTEP plot of the cation of **4** is shown in Figure 2 while structural data are given in Table 2.

The dimethylated form of HPTB (5,6-$Me_2$-HPTB) was synthesized in a similar way in order to improve the solubility of the resulting diiron(III) complexes in less polar organic

(47) Feig, A. L.; Bautista, M. T.; Lippard, S. J. *Inorg. Chem.* **1996**, *35*, 6892−6898.
(48) Nishida, Y.; Shimo, H.; Takahashi, K.; Kida, S. *Mem. Fac. Sci., Kyushu Univ., Ser. C* **1984**, *14*, 301−306.
(49) Ménage, S.; Brennan, B. A.; Juarez-Garcia, C.; Münck, E.; Que, L., Jr. *J. Am. Chem. Soc.* **1990**, *112*, 6423−6425.
(50) Tzou, J.-R.; Chang, S.-C.; Norman, R. E. *J. Inorg. Biochem.* **1993**, *51*, 480.
(51) Rardin, R. L.; Tolman, W. B.; Lippard, S. J. *New J. Chem.* **1991**, *15*, 417−430.
(52) Chen, Q.; Lynch, J. B.; Gomez-Romero, P.; Ben-Hussein, A.; Jameson, G. B.; O'Connor, C. J.; Que, L., Jr. *Inorg. Chem.* **1988**, *27*, 2673−2681.
(53) Ménage, S.; Que, L., Jr. *Inorg. Chem.* **1990**, *29*, 4293−4297.

**Table 2.** Selected Bond Lengths (Å) and Angles (deg) in **1**−**5**

(a) Bond Lengths in $[Fe_2(HPTB)(OH)(NO_3)_2]^{2+}$ (**1**)[50] and **2**, **3a**, **3b**, **4**, and **5**

| | **1** | **2** | **3a** | **3b** | **4** | **5** |
|---|---|---|---|---|---|---|
| Fe(1)···Fe(2) | 3.177(3) | 3.239(1) | 3.206(1) | 3.231(1) | 3.190(1) | 3.193(1) |
| Fe(1)−$O_{alkoxo}$ [O(1)] | 1.983(8) | 1.962(4) | 1.983(4) | 1.979(4) | 1.949(3) | 1.957(3) |
| Fe(2)−$O_{alkoxo}$ [O(1)] | 1.947(8) | 1.964(3) | 1.977(4) | 1.984(4) | 1.971(3) | 1.968(3) |
| Fe(1)−$O_{\mu-OH/\mu-OMe}$ [O(2)] | 1.985(8) | 2.021(3) | 1.983(4) | 1.976(4) | 1.981(3) | 1.968(3) |
| Fe(2)−$O_{\mu-OH/\mu-OMe}$ [O(2)] | 1.977(8) | 2.013(4) | 1.973(4) | 2.000(4) | 1.968(3) | 1.982(3) |
| Fe(1)−$O_{OBz/NO_3}$ [O(3)] | 2.066(10) | 2.050(4) | 1.988(4) | 2.002(4) | 2.049(4) | 2.069(3) |
| Fe(1)···$O_{OBz/NO_3}$ [O(4)] | | 2.927(4) | 2.821(5) | 2.883(5) | 2.854(4) | 3.022(4) |
| Fe(2)−$O_{OBz}(5)/O_{NO_3}(6)$ | 2.064(9) | 2.074(4) | 2.003(5) | 1.981(4) | 2.070(4) | 2.073(3) |
| Fe(2)···$O_{OBz}(6)/O_{NO_3}(7)$ | | 2.559(4) | 2.994(5) | 3.317(5) | 2.500(4) | 2.486(3) |
| Fe(1)−$N_{amine}$ [N(1)] | 2.39(1) | 2.372(4) | 2.423(5) | 2.412(5) | 2.354(4) | 2.367(3) |
| Fe(2)−$N_{amine}$ [N(2)] | 2.40(1) | 2.366(5) | 2.413(5) | 2.422(5) | 2.366(4) | 2.392(4) |
| Fe(1)−$N_{Bzim}$ [N(3)] | 2.08(1) | 2.046(4) | 2.109(5) | 2.082(5) | 2.051(4) | 2.030(3) |
| Fe(1)−$N_{Bzim}$ [N(5)] | 2.08(1) | 2.073(4) | 2.074(5) | 2.059(6) | 2.071(4) | 2.077(3) |
| Fe(2)−$N_{Bzim}$ [N(7)] | 2.02(1) | 2.074(5) | 2.063(5) | 2.038(5) | 2.058(4) | 2.089(4) |
| Fe(2)−$N_{Bzim}$ [N(9)] | 2.08(1) | 2.064(5) | 2.094(6) | 2.068(5) | 2.096(4) | 2.050(4) |

(b) Bond Angles in **2**, **3a**, **3b**, **4**, and **5**

| | **2** | **3a** | **3b** | **4** | **5** |
|---|---|---|---|---|---|
| Fe(1)−O(1)−Fe(2) | 111.2(2) | 108.0(2) | 109.3(2) | 108.9(2) | 108.9(1) |
| Fe(1)−O(2)−Fe(2) | 106.8(2) | 108.2(2) | 108.7(2) | 107.7(2) | 107.9(1) |
| O(1)−Fe(1)−O(2) | 70.8(1) | 71.4(2) | 71.3(2) | 71.7(1) | 71.9(1) |
| O(1)−Fe(1)−O(3) | 154.2(2) | 158.4(2) | 156.6(2) | 154.1(1) | 150.4(1) |
| O(1)−Fe(1)−N(1) | 73.7(1) | 74.2(2) | 75.0(2) | 73.7(1) | 73.2(1) |
| O(1)−Fe(1)−N(3) | 106.5(2) | 94.3(2) | 90.4(2) | 99.6(2) | 104.9(1) |
| O(1)−Fe(1)−N(5) | 98.3(2) | 102.7(2) | 100.8(2) | 103.0(1) | 101.6(1) |
| O(2)−Fe(1)−O(3) | 84.9(1) | 89.0(2) | 86.8(2) | 82.6(1) | 80.7(1) |
| O(2)−Fe(1)−N(1) | 143.7(2) | 144.4(2) | 145.6(2) | 144.7(1) | 143.0(1) |
| O(2)−Fe(1)−N(3) | 107.7(2) | 115.5(2) | 111.8(2) | 104.2(2) | 102.8(1) |
| O(2)−Fe(1)−N(5) | 118.9(2) | 105.2(2) | 106.2(2) | 120.4(1) | 124.7(1) |
| O(3)−Fe(1)−N(1) | 131.3(2) | 126.3(2) | 127.5(2) | 132.2(1) | 135.8(1) |
| O(3)−Fe(1)−N(3) | 88.9(2) | 85.7(2) | 90.4(2) | 89.2(2) | 91.5(1) |
| O(3)−Fe(1)−N(5) | 85.5(2) | 91.0(2) | 92.7(2) | 87.4(2) | 85.0(1) |
| N(1)−Fe(1)−N(3) | 75.2(2) | 75.7(2) | 74.8(2) | 75.1(2) | 75.1(1) |
| N(1)−Fe(1)−N(5) | 73.6(2) | 73.7(2) | 73.4(2) | 74.1(1) | 74.0(1) |
| N(3)−Fe(1)−N(5) | 132.2(2) | 139.1(2) | 142.0(2) | 134.3(2) | 130.8(1) |
| O(1)−Fe(2)−O(2) | 70.9(1) | 71.8(2) | 70.6(2) | 71.5(1) | 71.3(1) |
| O(1)−Fe(2)−$O_{OBz}(5)/O_{NO_3}(6)$ | 154.5(2) | 158.0(2) | 154.7(2) | 151.2(1) | 149.3(1) |
| O(1)−Fe(2)−N(2) | 75.9(2) | 73.7(2) | 73.0(2) | 74.7(1) | 74.7(1) |
| O(1)−Fe(2)−N(7) | 99.8(2) | 95.0(2) | 100.5(2) | 101.5(1) | 89.6(1) |
| O(1)−Fe(2)−N(9) | 89.7(2) | 98.4(2) | 100.2(2) | 88.5(1) | 99.7(1) |
| O(2)−Fe(2)−$O_{OBz}(5)/O_{NO_3}(6)$ | 84.6(1) | 86.2(2) | 84.4(2) | 82.9(2) | 80.8(1) |
| O(2)−Fe(2)−N(2) | 146.4(1) | 145.5(2) | 143.3(2) | 144.4(1) | 143.8(1) |
| O(2)−Fe(2)−N(7) | 104.3(2) | 105.9(2) | 108.0(2) | 101.3(1) | 116.2(1) |
| O(2)−Fe(2)−N(9) | 108.8(2) | 114.0(2) | 118.5(2) | 113.5(1) | 98.3(1) |
| $O_{OBz}(5)/O_{NO_3}(6)$−Fe(2)−N(2) | 128.9(2) | 128.3(2) | 132.2(2) | 132.5(1) | 134.9(1) |
| $O_{OBz}(5)/O_{NO_3}(6)$−Fe(2)−N(7) | 93.0(2) | 90.7(2) | 90.8(2) | 96.1(2) | 91.3(1) |
| $O_{OBz}(5)/O_{NO_3}(6)$−Fe(2)−N(9) | 91.4(2) | 90.6(2) | 88.0(2) | 90.0(2) | 96.7(1) |
| N(2)−Fe(2)−N(7) | 75.8(2) | 75.4(2) | 73.9(2) | 74.9(1) | 75.3(1) |
| N(2)−Fe(2)−N(9) | 76.0(2) | 72.8(2) | 72.7(2) | 75.9(1) | 75.4(1) |
| N(2)−Fe(2)−N(9) | 146.9(2) | 140.1(2) | 133.1(2) | 145.2(2) | 145.5(1) |

solvents. This ligand has been used before to prepare the corresponding diiron(III) complex, and its reaction with hydrogen peroxide has been investigated.[28] However, efforts to synthesize and crystallographically characterize this complex were unsuccessful, and only tetranuclear complexes with this ligand were reported.[52] In contrast to these earlier studies we could synthesize and structurally characterize the dinuclear iron(III) complex with 5,6-$Me_2$-HPTB as ligand.

The cation of $[Fe_2(5,6\text{-}Me_2\text{-}HPTB)(\mu\text{-}OH)(NO_3)_2](ClO_4)(NO_3)\cdot 3.5CH_3OH\cdot C_2H_5OC_2H_5\cdot 0.5H_2O$ (**5**) is shown in Figure S2 (Supporting Information), and structural details are presented in Table 2.

The structures of **4** and **5** are very similar to each other and strongly related to those of **1**−**3**. All four compounds described here reveal a structurally similar $Fe_2(\mu\text{-alkoxo})(\mu\text{-OR})(OR')_2$ core. This similarity includes all characteristic structural features of the central structural motif. This is due to the close relationship of the used ligands HPTB, N-EtOH-HPTB, and 5,6-$Me_2$-HPTB, which all reveal benzimidazole units and due to the comparable synthetic conditions.

Additional efforts to introduce further bridging groups such as pyrazole into the dinuclear iron core lead to interesting results. From a mixture of iron(III) perchlorate, pyrazole, HPTB, and sodium tetrafluoroborate in acetonitrile the tetranuclear complex $[Fe_4(HPTB)_2(\mu\text{-}F)_2(OH)_4](ClO_4)_4\cdot CH_3CN\cdot C_2H_5OC_2H_5\cdot H_2O$ (**6**) was obtained instead of a dinuclear species. A plot of the molecular structure of the cation in **6** is shown in Figure 3, and structural details are given in Table 3.

The cation of compound **6** in which all four iron atoms have a distorted octahedral environment with the $N_3O_2F$-donor set can be regarded as a dimer of two $[Fe_2(HPTB)(OH)_2]^{3+}$ units linked by two nearly linear fluoro bridges. The ligand HPTB chelates each iron(III) ion by two benzimidazole nitrogen atoms, one tertiary amine nitrogen, and a bridging alkoxo oxygen atom.

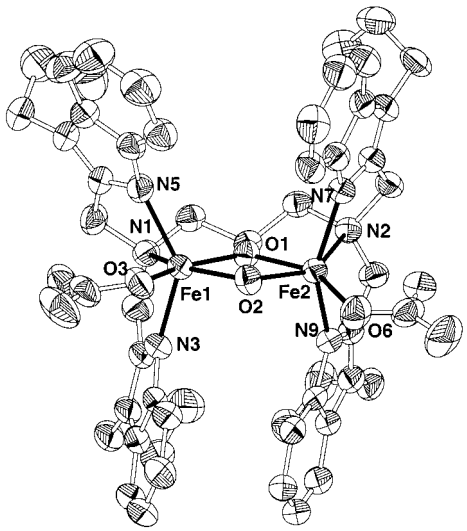


**Figure 2.** Structure of the cation in **4** showing 50% probability ellipsoids; hydrogen atoms have been omitted for clarity.

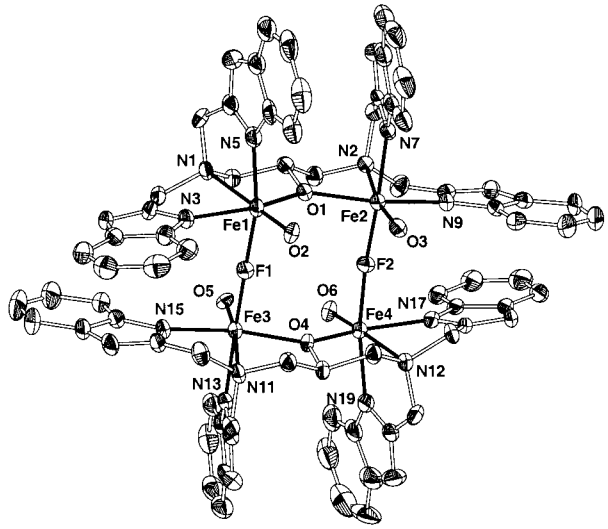


**Figure 3.** Structure of the cation in **6** showing 50% probability ellipsoids; hydrogen atoms have been omitted for clarity.

Additionally, one terminal hydroxo ligand and a fluoro bridge are coordinated to each iron ion.

Interestingly complex **6** contains two fluoride anions. These fluoride anions are derived from the hydrolysis of tetrafluoroborate. Similar reactions have been reported in the literature.[54,55] Compound **6** is the first reported double fluoro-bridged tetranuclear iron(III) complex. The mixed-valent tetranuclear Fe$_4$(II,III,II,III) complex [Fe$_4$(Me$_4$-tpdp)$_2$($\mu$-F)$_2$(OH)$_2$(H$_2$O)$_2$](BF$_4$)$_4$ (HMe$_4$-tpdp = *N*,*N*,*N*′,*N*′-tetrakis[2-(6-methylpyridyl)-methyl]-2-hydroxo-1,3-diaminopropane) has been published recently, in which the fluoro ligands in contrast to the synthesis of **6** were directly added as the sodium salt to the solution.[54] Due to the mixed-valent character only the iron(III) moiety can be compared to **6**. The Fe−F bond lengths in **6** have an average value of 1.966 Å, whereas the Fe(III)−F distance in the mixed-valent species is 1.938(8) Å. In comparison, the usually observed Fe(III)−F$_{terminal}$ distances are significantly longer.[56] Due to the lack of an additional bridging ligand the iron centers of each dinuclear unit in **6** show long metal−metal distances [Fe(1)···Fe(2) 3.671(2) Å, Fe(3)···Fe(4) 3.640(2) Å] compared to those values we observed for the dinuclear iron(III) complexes **2**−**5**. In analogy to compounds **2**−**5**, the averaged Fe−N$_{amine}$ distance in **6** of 2.287 Å is significantly longer than the averaged Fe−N$_{Bzim}$ bond lengths of 2.094 Å. This difference is characteristic for benzimidazole containing iron(III) complexes and can be explained by structural constraints imposed by the incorporation of imidazole rings into a five-membered chelate ring. All structurally characterized compounds in this paper show this feature.

Compound **6** shows an interesting difference in the cationic structure compared to those observed for compounds **2**−**5**. In complex **6**, the two benzimidazole groups of each octahedral coordination sphere of the iron(III) centers are cis-orientated to each other, while in **2**−**5**, the N$_{Bzim}$-donor atoms coordinate trans to the iron(III) ions. We have observed analogous equatorial positions for the nitrogen donor atoms of the benzimidazole moieties in the crystal structures of diiron(III) complexes in which additional ligands such as phosphate or cacodylate are

**Table 3.** Selected Bond Lengths (Å) and Angles (deg) in **6**

(a) Bond Lengths

| | | | |
|---|---|---|---|
| Fe(1)···Fe(2) | 3.671(2) | Fe(2)···Fe(4) | 3.924(2) |
| Fe(1)···Fe(3) | 3.930(2) | Fe(3)···Fe(4) | 3.640(2) |
| Fe(1)−O(1) | 2.006(4) | Fe(3)−O(4) | 2.020(4) |
| Fe(1)−O(2) | 1.817(4) | Fe(3)−O(5) | 1.817(4) |
| Fe(1)−F(1) | 1.965(4) | Fe(3)−F(1) | 1.968(4) |
| Fe(1)−N(1) | 2.296(5) | Fe(3)−N(11) | 2.280(5) |
| Fe(1)−N(3) | 2.107(5) | Fe(3)−N(13) | 2.074(5) |
| Fe(1)−N(5) | 2.080(5) | Fe(3)−N(15) | 2.117(5) |
| Fe(2)−O(1) | 2.037(4) | Fe(4)−O(4) | 2.007(4) |
| Fe(2)−O(3) | 1.813(4) | Fe(4)−O(6) | 1.804(4) |
| Fe(2)−F(2) | 1.954(4) | Fe(4)−F(2) | 1.976(4) |
| Fe(2)−N(2) | 2.276(5) | Fe(4)−N(12) | 2.297(5) |
| Fe(2)−N(7) | 2.067(5) | Fe(4)−N(17) | 2.088(5) |
| Fe(2)−N(9) | 2.130(5) | Fe(4)−N(19) | 2.085(5) |

(b) Bond Angles

| | | | |
|---|---|---|---|
| Fe(1)−O(1)−Fe(2) | 130.5(2) | Fe(3)−O(4)−Fe(4) | 129.4(2) |
| Fe(1)−F(1)−Fe(3) | 175.7(2) | Fe(2)−F(2)−Fe(4) | 174.0(2) |
| O(1)−Fe(1)−O(2) | 105.7(2) | O(4)−Fe(3)−O(5) | 106.3(2) |
| O(1)−Fe(1)−F(1) | 88.4(2) | O(4)−Fe(3)−F(1) | 88.5(2) |
| O(1)−Fe(1)−N(1) | 80.0(2) | O(4)−Fe(3)−N(11) | 79.8(2) |
| O(1)−Fe(1)−N(3) | 154.1(2) | O(4)−Fe(3)−N(13) | 89.7(2) |
| O(1)−Fe(1)−N(5) | 94.0(2) | O(4)−Fe(3)−N(15) | 154.5(2) |
| O(2)−Fe(1)−F(1) | 94.9(2) | O(5)−Fe(3)−F(1) | 95.4(2) |
| O(2)−Fe(1)−N(1) | 172.5(2) | O(5)−Fe(3)−N(11) | 172.3(2) |
| O(2)−Fe(1)−N(3) | 99.5(2) | O(5)−Fe(3)−N(13) | 96.7(2) |
| O(2)−Fe(1)−N(5) | 97.4(2) | O(5)−Fe(3)−N(15) | 99.1(2) |
| F(1)−Fe(1)−N(1) | 90.1(2) | F(1)−Fe(3)−N(11) | 89.6(2) |
| F(1)−Fe(1)−N(3) | 83.5(2) | F(1)−Fe(3)−N(13) | 167.9(2) |
| F(1)−Fe(1)−N(5) | 166.4(2) | F(1)−Fe(3)−N(15) | 86.2(2) |
| N(1)−Fe(1)−N(3) | 75.4(2) | N(11)−Fe(3)−N(13) | 78.3(2) |
| N(1)−Fe(1)−N(5) | 77.2(2) | N(11)−Fe(3)−N(15) | 75.2(2) |
| N(3)−Fe(1)−N(5) | 88.6(2) | N(13)−Fe(3)−N(15) | 90.3(2) |
| O(1)−Fe(2)−O(3) | 109.0(2) | O(4)−Fe(4)−O(6) | 106.5(2) |
| O(1)−Fe(2)−F(2) | 88.1(2) | O(4)−Fe(4)−F(2) | 87.8(2) |
| O(1)−Fe(2)−N(2) | 80.0(2) | O(4)−Fe(4)−N(12) | 80.0(2) |
| O(1)−Fe(2)−N(7) | 89.6(2) | O(4)−Fe(4)−N(17) | 153.6(2) |
| O(1)−Fe(2)−N(9) | 153.6(2) | O(4)−Fe(4)−N(19) | 94.3(2) |
| O(3)−Fe(2)−F(2) | 94.6(2) | O(6)−Fe(4)−F(2) | 95.3(2) |
| O(3)−Fe(2)−N(2) | 170.1(2) | O(6)−Fe(4)−N(12) | 170.9(2) |
| O(3)−Fe(2)−N(7) | 97.0(2) | O(6)−Fe(4)−N(17) | 99.3(2) |
| O(3)−Fe(2)−N(9) | 97.2(2) | O(6)−Fe(4)−N(19) | 95.4(2) |
| F(2)−Fe(2)−N(2) | 89.8(2) | F(2)−Fe(4)−N(12) | 91.2(2) |
| F(2)−Fe(2)−N(7) | 168.3(2) | F(2)−Fe(4)−N(17) | 84.3(2) |
| F(2)−Fe(2)−N(9) | 86.8(2) | F(2)−Fe(4)−N(19) | 168.0(2) |
| N(2)−Fe(2)−N(7) | 78.5(2) | N(12)−Fe(4)−N(17) | 75.1(2) |
| N(2)−Fe(2)−N(9) | 74.2(2) | N(12)−Fe(4)−N(19) | 77.6(2) |
| N(7)−Fe(2)−N(9) | 90.2(2) | N(17)−Fe(4)−N(19) | 88.7(2) |

(54) Ghiladi, M.; McKenzie, C. J.; Meier, A.; Powell, A. K.; Ulstrup, J.; Wocadlo, S. *J. Chem. Soc., Dalton Trans.* **1997**, 4011−4018.
(55) Ghiladi, M.; Jensen, K. B.; Jiang, J.; McKenzie, C. J.; Morup, S.; Sotofte, I.; Ulstrup, J. *J. Chem. Soc., Dalton Trans.* **1999**, 2675−2681.
(56) Sugimoto, H.; Hayashi, Y.; Koshi, C.; Fujinami, S.; Suzuki, M.; Maeda, Y.; Uehara, A. *Chem. Lett.* **1996**, 933−934.

bound in a bidentate mode to the iron atoms.[32,37,40,57] This observation is due to steric and geometrical reasons. The additional dimer-bridging $\mu$-fluoro ligands in **6** as well as additional bridging phosphate or cacodylate ligands force the benzimidazole residues to a cis-orientated coordination. Complexes **2**−**5** contain each two terminal nitrate or benzoate ligands and only one bridging $\mu$-hydroxo group. The observed coordination modes of the nitrate and benzoate groups cause a minimum of steric hindrance between the additional nonbridging nitrate or benzoate. As a consequence, the benzimidazole groups in **2**−**5** are trans-orientated.

**Stability and Reactivity of Dioxygen Adducts.** As described above, hydrogen peroxide reacts irreversibly with iron(III) complexes of HPTB to form peroxo complexes.[28,29] Therefore, complexes such as **1** can be used for the quantitative detection of hydrogen peroxide.[33,34] **1** has a very high affinity toward peroxide; the stoichiometry of this reaction is 1:1. $K'_{\mathrm{eff}}$ for this reaction in methanol was estimated to be greater than $10^6$ $M^{-1}$.[28] A $^1$H NMR titration showed that the peroxide species is completely formed when 1 equiv of $H_2O_2$ was added to **1**.[28] A resonance Raman study revealed that neither of the peroxide oxygen atoms is protonated; this observation was supported by the crystal structure of the diiron(III) peroxo complex containing the ligand N-Et-HPTB.[25,28]

Because of the very fast reaction of **1** with hydrogen peroxide the formation of the diiron(III) peroxo adduct is best followed spectrophotometrically with stopped-flow techniques. A mechanism in buffered aqueous solution was recently suggested by some of us.[40]

The ligands N-EtOH-HPTB and 5,6-$Me_2$-HPTB were synthesized in order to improve the solubility of the iron(III) complexes in various solvents. Furthermore, these ligands allowed the investigation of the effects on the reactivity of **1** when different substituents were introduced into the ligand backbone of HPTB. While **4** is more soluble in aqueous solution than **1** and therefore could be investigated under identical conditions, **5**, however, was insoluble.

Time-resolved spectra observed during the reaction of **4** with an excess of hydrogen peroxide are shown in Figure S3a at pH 3.00 and in Figure S3b at pH 4.50 (Supporting Information). The kinetic data were treated with a global analysis fitting routine (using the program Specfit) and/or by extracting single absorbance vs time traces at different wavelengths. These traces were fitted to single-exponential functions. Plots of the obtained pseudo-first-order rate constants $k_{\mathrm{obs}}$ vs the hydrogen peroxide concentration exhibited a linear dependence without an intercept. Therefore, the overall second-order rate law can be expressed as $\mathrm{d[peroxo\ complex]/d}t = k[\mathbf{4}][H_2O_2]$ (second-order rate constants at 25 °C: pH = 3.00, 1459 ± 73 $M^{-1}$ $s^{-1}$; pH = 3.50, 2328 ± 116 $M^{-1}$ $s^{-1}$; pH = 4.00, 3041 ± 152 $M^{-1}$ $s^{-1}$; pH = 4.50, 4000 ± 150 $M^{-1}$ $s^{-1}$). The reaction of **4** with hydrogen peroxide is slightly pH-dependent as observed previously for the reaction of **1**.[58] This is presumably caused by the deprotonation of a ligand in the coordination sphere of the complex at higher pH resulting in an increase of reactivity. This assumption is supported by the variation of the UV−vis spectra of **1** and **4** with pH: the absorbance maxima of **1** and **4** shift to lower wavelengths with increasing pH. Spectrophotometric titrations were performed with both complexes, but the obtained data could not be resolved due to the complexity of the system.

(57) Krebs, B.; Klabunde, T.; Sträter, N.; Witzel, H.; Than, R.; Sift, B. *J. Inorg. Biochem.* **1997**, *67*, 322.
(58) Higher pH values caused precipitation of the complexes under these conditions.

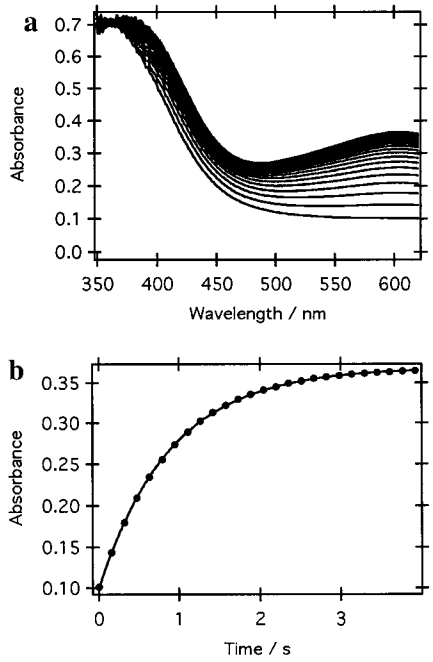


**Figure 4.** (a) Time-resolved spectra ($\Delta t = 0.15$ s) for the reaction of **4** with an excess of $H_2O_2$ in methanol. Experimental conditions: [**4**] = $1 \times 10^{-4}$ M, $T = 25.0$ °C, $[H_2O_2] = 6 \times 10^{-3}$ M. (b) Absorbance vs time trace at 600 nm (data points and fit).

The differences in the UV−vis spectra can be observed in the time-resolved spectra of the reaction of hydrogen peroxide with **4** as well; at pH 3.00 (Figure S3a) isosbestic points are observed which disappear at higher pH (pH 4.50, Figure S3b). Furthermore, the temperature dependence of this reaction at pH 3.00 was measured. The analysis according to the Eyring equation allowed the calculation of the activation parameters $\Delta H^{\ddagger} = 55 \pm 1$ kJ/mol and $\Delta S^{\ddagger} = 0 \pm 3$ J/(mol K).

The reactions of **1** and **4** with hydrogen peroxide showed identical rates within error.[40] From this finding it is clear that substitution of the protons of the benzimidazole units of HPTB in complex **1** with N-EtOH groups does not affect the reaction behavior toward hydrogen peroxide. We suggest that both complexes react with hydrogen peroxide in aqueous solution according to the mechanism postulated earlier.[40]

When hydrogen peroxide was added to **1** in a variety of solvents including water, the color changed from yellow-orange to blue-green with the final color showing solvent dependence ($\lambda_{\mathrm{max}}$ = 560 nm ($\epsilon$ = 2200 $M^{-1}$ $cm^{-1}$) in water and 604 nm (1600 $M^{-1}$ $cm^{-1}$) in methanol).[28] Furthermore, the stability of the peroxo complex formed during the reaction of the iron(II) HPTB compound with dioxygen could be enhanced strongly when acetonitrile/dmso mixtures were used.[28] For a better understanding of these effects we used **1**, **4**, and **5** to investigate the reaction behavior toward hydrogen peroxide in organic solvents. Because all three complexes react very similarly with identical rate constants within error, only the reaction of **4** with hydrogen peroxide in methanol, acetonitrile, and dmso will be discussed in the following section.

The reaction of **4** with hydrogen peroxide in methanol was studied under pseudo-first-order conditions ($[H_2O_2] \gg$ [complex]). Absorbance time traces extracted from the time-resolved spectra (Figure 4a) could be fitted to single-exponential functions (Figure 4b shows data points and fit).

A plot of the obtained pseudo-first-order rate constants $k_{\mathrm{obs}}$ vs hydrogen peroxide concentration at different temperatures

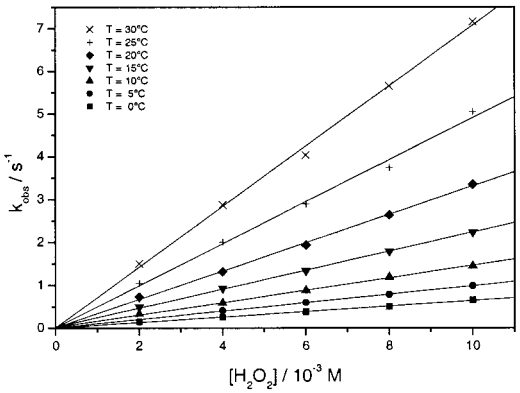


**Figure 5.** Plot of the pseudo-first-order rate constants $k_{obs}$ vs hydrogen peroxide concentration at different temperatures.

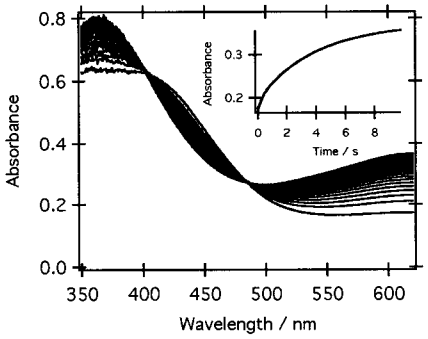


**Figure 6.** Time-resolved spectra ($\Delta t = 0.3$ s) for the reaction of **4** with an excess of $H_2O_2$ in acetonitrile. Experimental conditions: [**4**] $= 1 \times 10^{-4}$ M, $T = 25.0$ °C, $[H_2O_2] = 6 \times 10^{-3}$ M.

exhibited linear dependences without intercepts (Figure 5) similar to the findings described above for the aqueous solutions. Activation parameters were calculated from an Eyring plot (second-order rate constants: $65 \pm 1$ $M^{-1}$ $s^{-1}$ at 0 °C; $99 \pm 1$ $M^{-1}$ $s^{-1}$ at 5 °C; $147 \pm 25$ $M^{-1}$ $s^{-1}$ at 10 °C; $225 \pm 16$ $M^{-1}$ $s^{-1}$ at 15 °C; $331 \pm 50$ $M^{-1}$ $s^{-1}$ at 20 °C; $490 \pm 15$ $M^{-1}$ $s^{-1}$ at 25 °C; $707 \pm 15$ $M^{-1}$ $s^{-1}$ at 30 °C) to $\Delta H^{\#} = 53 \pm 3$ kJ/mol and $\Delta S^{\#} = -17 \pm 1$ J/molK.

The reaction behavior in methanol and aqueous solutions is similar, but the reaction in aqueous solution is faster by a factor of 3−8 at 25 °C (depending on the pH in the range 3.0−4.5). The time-resolved spectra for the reaction of **4** with hydrogen peroxide in aqueous solution at pH 4.50 (Figure S3b) are similar to those obtained in methanol (no isosbestic points are observed), but the absorbance maximum is shifted to a higher wavelength in methanol.

Time-resolved UV−vis spectra for the reaction of **4** with excess hydrogen peroxide in acetonitrile are shown in Figure 6. Compared to methanolic solutions the absorbance maximum in acetonitrile was shifted toward higher wavelengths, and, furthermore, isosbestic points were observed.

Absorbance time traces were fitted reasonably well to single-exponential functions; a plot of the obtained pseudo-first-order rate constants $k_{obs}$ vs hydrogen peroxide concentration shows a linear dependence with no or a very small intercept. A better fit, however, was obtained when the data were calculated with the sum of two (inset in Figure 6) or three exponential functions. The observed rate constants for the slower reaction were very similar to the ones obtained from the fit to a single-exponential function. These data were used to calculate the second-order rate constant ($k = 115 \pm 10$ $M^{-1}$ $s^{-1}$ at 25 °C) which is smaller than the one obtained from the measurements in methanol. Unfortunately, the observed rate constants for the faster reactions could not be accurately determined.

In dmso, the reaction behavior of **4** toward hydrogen peroxide was quite different. Isosbestic points were not observed in the time-resolved spectra (Figure S4a, Supporting Information), and absorbance time traces could be fitted reasonably well to single-exponential functions (Figure S4b). But here a plot of the obtained pseudo-first-order rate constants $k_{obs}$ vs $[H_2O_2]$ exhibited a linear dependence with an intercept. Therefore, the rate law can be written as $d[\text{peroxo complex}]/dt = k_a[\mathbf{4}] + k_b[\mathbf{4}][H_2O_2]$ ($k_a = 0.0036 \pm 0.0005$ $s^{-1}$; $k_b = 3.0 \pm 0.3$ $M^{-1}$ $s^{-1}$ at 25 °C). The second-order rate constant is much smaller compared to those obtained for the other solvents. Furthermore, an additional reaction pathway, independent of the hydrogen peroxide concentration, is observed.

The variations in the reaction behavior of the dinuclear iron(III) complexes toward hydrogen peroxide in different solvents are caused by the additional ligands S and T in **1**, **4**, and **5** (Scheme 1). In aqueous solution the nitrate anions (= S and T), which are coordinated in the solid state, are replaced by water molecules: the protic solvent is able to compensate the positive charge of +4 of the cation by hydrogen bonding and allows the replacement of the nitrate ions. This was confirmed by conductivity measurements of **1** and **4** which clearly showed that these compounds behave as 1:4 electrolytes.

Therefore, in aqueous solutions S and T represent water molecules. As discussed before for the reaction of **1**,[40] also for **4** the first reaction step, the rate-determining substitution of a water molecule through hydrogen peroxide, is followed by the fast second step, the ring closure. The activation parameters for the reaction of **4** with $H_2O_2$ support this mechanism. The values of almost zero for the activation entropy and activation volume for **4** and **1** are typical for a pure interchange mechanism, where coordinated water is displaced during the first step.[40] According to this mechanism the variation of ionic strength should not have any effect on the rate of the reaction since hydrogen peroxide is a neutral molecule. This was indeed detected by our measurements at different ionic strengths (adjusted with sodium nitrate up to 0.5 M).

In pure organic solvents, anions are coordinated much stronger to the iron(III) ions, which was confirmed by conductivity measurements for **1** in acetonitrile showing coordination of the nitrate ions (S = T = $NO_3^-$ in Scheme 1).[28] Furthermore, they can compete successfully with other ligands; for example, they replace coordinated benzoate in **3**.[50] Substitution of these coordinated nitrate anions with neutral molecules is less favorable than the replacement of water molecules in aqueous solution.

With hydrogen peroxide as a reactant the introduction of water into the organic solvent cannot be avoided; also, the complexes contain different amounts of water molecules from crystallization. This can be critical for the exact determination of the rate constants. When additional water was added to solutions of the complex in organic solvents, the reaction became faster. We tried to avoid this problem by deliberately adding excess constant amounts of water. However, this caused serious problems with data fitting of the measured absorbance/time data. Finally, best results were obtained when we used very small amounts of hydrogen peroxide and a minute amount of water to keep the overall water content constant.

The expectation that coordinated nitrate anions are replaced by water molecules in organic solvents if additional water is present was not fulfilled. Instead, the solvation of the complexes varies and S and T (S, T = nitrate, water, or organic solvent

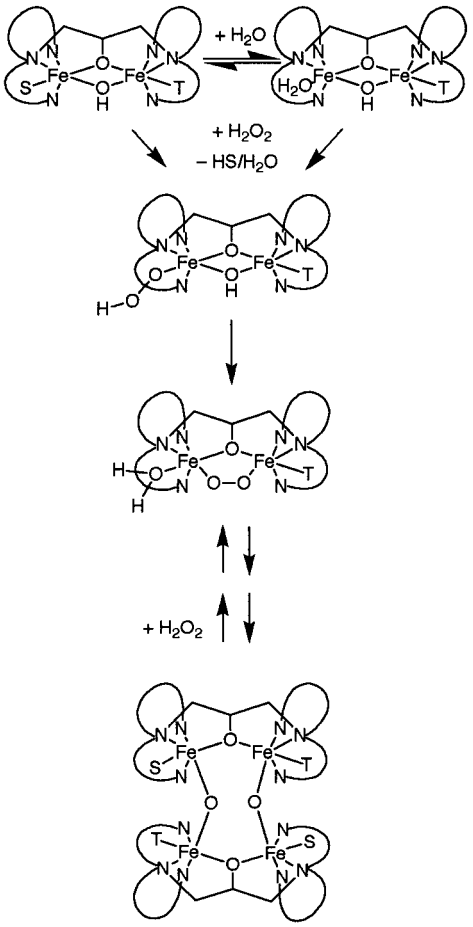


**Figure 7.** Postulated mechanism for the reaction of **1**, **4**, and **5** with hydrogen peroxide in different solvents (charges are omitted).

molecule) play a crucial role in the reaction behavior of the complexes. Additional pathways were observed for the reaction of the iron(III) complexes with hydrogen peroxide in organic solvents in contrast to the simple mechanism observed in aqueous solutions (Figure 7).

In dmso, a strongly coordinating ligand for iron(III), it most likely replaces the nitrate anions when **4** is dissolved. Therefore, the substitution of coordinated dmso with hydrogen peroxide is very slow. In an alternative pathway, the coordinated dmso is substituted by a water molecule (or nitrate) in the rate-determining step prior to the reaction with hydrogen peroxide (first reaction in Figure 7). This leads to a rate constant that is independent of the hydrogen peroxide concentration (intercept in plot of $k_{obs}$ vs $[H_2O_2]$ discussed above).

To confirm that dmso is coordinated to **4** instead of water molecules or nitrate anions, we isolated crystals from solutions of **4** in dmso. But instead of obtaining **4** with ligated dmso we found that N-EtOH-HPTB was completely replaced by dmso molecules which lead to $[Fe(III)(dmso)_6](NO_3)_3$. The crystal structure of this complex was obtained but found to be identical to the one described earlier.[59]

From the kinetic findings we suggest the mechanism shown in Figure 7 for the reaction of **1**, **4**, and **5** with hydrogen peroxide. In aqueous solutions $S = T = H_2O$ and the mechanism is identical to one suggested earlier. But in organic solvents T and S can be $H_2O$, $NO_3^-$, or organic solvent molecule. Therefore, additional reactions can occur as discussed above.

These findings also explain the stabilization of the peroxo complexes in different solvents. If S and T are strongly coordinating ligands such as dmso or $Ph_3PO$, the iron(III) complex is nearly inert to substitution and therefore the decomposition of the peroxo complex becomes very slow. This was proved when the peroxo complex $[Fe_2(N\text{-Et-HPTB})(O_2)(Ph_3PO)_2]^{3+}$ was isolated and structurally characterized.[25]

Furthermore, during the present investigations we tried to resolve the question of why peroxo complexes obtained from the reaction of the dinuclear iron(II) complexes with dioxygen seemed to be less stable (very short lifetime)[26] than those obtained from the reaction of the analogous iron(III) complexes with hydrogen peroxide (stable for hours). Formation of the peroxo complexes is irreversible and does not depend on the way of its formation. Therefore, differences between the reaction pathways of the iron(II) complexes with dioxygen and those of the iron(III) complexes with hydrogen peroxide cannot be the reason for the different stabilities. Instead, we propose that the final products of the decomposition reactions of the peroxo complexes are responsible for this effect. These products are tetranuclear oxo-bridged iron(III) complexes; one of these products with additional bridging benzoate ligands was structurally characterized earlier.[52]

A bridging benzoate ligand is not necessarily required for the formation of such a tetranuclear species; instead, other groups can be coordinated as monodentate ligands. We were able to obtain the tetranuclear oxo-bridged iron(III) complex $[Fe_4(HPTB)_2(\mu\text{-}O)_2(OH)_4](NO_3)_2 \cdot 6CH_3OH \cdot 2H_2O$ (tetranuclear complex in Figure 7, $S = T = OH^-$), which was synthesized by the addition of small amounts of $NEt_3$ to a methanolic solution of **1** (depending on the conditions $[Fe_4(HPTB)_2(\mu\text{-}O)_2(OH)_4](NO_3)_2 \cdot 6CH_3OH \cdot 2H_2O$ or **2** was formed). Unfortunately, the crystal structure analysis of this tetranuclear complex displayed high disorder. But the stoichiometry and structure of the species was established.[60] The structure of this complex is very similar to the fluoride-bridged complex **6** described above, with the fluoride bridges replaced by oxo bridges.

We observed that the orange tetranuclear complexes react with hydrogen peroxide to re-form blue peroxo compounds. This reaction is reversible and, therefore, peroxo complexes prepared from an excess of hydrogen peroxide and iron(III) complexes are stable for hours in contrast to those prepared from iron(II) complexes and dioxygen. If no hydrogen peroxide is present, the peroxo complexes decompose very fast. Furthermore, adding hydrogen peroxide to a solution of decomposed iron peroxo complexes formed from iron(II) and dioxygen caused re-formation of blue peroxo species as well. We propose that these peroxo complexes are dinuclear but cannot exclude the possibility that polynuclear peroxo species form in an analogous manner to those reported for copper complexes.[61]

## Summary

This work describes the syntheses and structural characterization of a series of new iron(III) complexes and their reactions with hydrogen peroxide in various solvents. Each compound

(59) Tzou, J.-R.; Mullaney, M.; Norman, R. E.; Chang, S.-C. *Acta Crystallogr.* **1995**, *C51*, 2249−2252.

(60) Schmidt, M. Ph.D. Thesis, University of Münster, 1996. The complex crystallizes in the triclinic space group P$\bar{1}$ with cell constants $a$ = 12.898(8) Å, $b$ = 13.908(6) Å, $c$ = 14.472(6) Å, $\alpha$ = 77.11(1)°, $\beta$ = 77.89(1)°, $\gamma$ = 68.54(1)°, $V$ = 2331.6(29) Å$^3$. The data could be fitted to final $R$ values R1 = 0.124 and wR2 = 0.343 for $I > 2\sigma(I)$.

(61) Lee, D. H.; Wie, N.; Murthy, N. N.; Tyeklar, Z.; Karlin, K. D.; Kaderli, S.; Jung, B.; Zuberbuhler, A. D. *J. Am. Chem. Soc.* **1995**, *117*, 12498−12513.

(62) Bremer, B.; Schepers, K.; Fleischauer, P.; Haase, W.; Henkel, G.; Krebs, B. *J. Chem. Soc., Chem. Commun*. **1991**, 510−512.

contains terminally coordinated benzoato (**3**) or nitrato (**2**, **4**, and **5**) ligands. Compound **3** is the first structurally characterized diiron(III) complex with a dinucleating ligand as well as additional nonbridging benzoato ligands. Compound **5** is the first structurally characterized diiron(III) complex with the ligand 5,6-$Me_2$-HPTB. The tetranuclear iron(III) complex **6** consists of two $[Fe_2L(OH)_2]$ units that are connected by nearly linear fluoro bridges. It is the first reported structurally characterized fluoro-bridged tetrairon(III) complex.

The present kinetic investigations give clear evidence of the mechanism for the reaction of the dinuclear iron(III) complexes **1**, **4**, and **5** with hydrogen peroxide. It could be shown why these reactions proceed with very different reaction rates in various solvents and why the peroxo complexes are most persistent when dmso or other strongly coordinating ligands are present. Furthermore, it is possible to explain why the iron peroxo complexes formed from the iron(III) precursors seem to be more stable than the same complexes formed from iron(II) complexes and dioxygen.

**Acknowledgment.** The authors gratefully acknowledge financial support from the Volkswagen-Stiftung. Prof. István Fábián (University of Debrecen, Hungary) is acknowledged for his efforts in performing the titration experiments and for worthful discussions. B.K. thanks the Deutsche Forschungsgemeinschaft, the Fonds der Chemischen Industrie, the Henkel KGaA, and the Degussa AG for generous financial support. S.S. furthermore would like to thank Prof. Dr. Rudi van Eldik (University of Erlangen-Nürnberg) for his support of this work.

**Supporting Information Available:** Figures S1−S4 and listings of complete CIF files for **2**−**6**. This material is available free of charge via the Internet at http://pubs.acs.org. Crystallographic data (excluding structural factors) for **2**−**6** have been deposited as supplementary publication no. CCDC-139030 (**2**), -139029 (**3**), -139031 (**4**), -139032 (**5**), and -139033 (**6**) at the Cambridge Crystallographic Data Centre. Copies can be obtained free of charge from The Director, CCDC, 12 Union Road, Cambridge CB21 EZ, U.K. (fax, +44-1223-336-033; e-mail, deposit@ccdc.cam.ac.uk).

IC0009371